ELSEVIER

www.elsevier.nl/locate/jphotobiol

J. Photochem. Photobiol. B: Biol. 53 (1999) 44–52

Journal of Photochemistry and Photobiology B:Biology

Photodynamic parameters in the chick chorioallantoic membrane (CAM) bioassay for topically applied photosensitizers

Marie J. Hammer-Wilson [a], Lori Akian [a], Jenny Espinoza [a], Sol Kimel [a,b], Michael W. Berns [a,*]

[a] *Beckman Laser Institute and Medical Clinic, University of California, Irvine, CA 92612, USA*
[b] *Department of Chemistry, Technion-Israel Institute of Technology, Haifa, 32000, Israel*

Received 18 June 1999; accepted 14 October 1999

Abstract

The relative efficacy of Photofrin®-based photodynamic therapy (PDT) has been compared with that of the second-generation photosensitizers 5-aminolevulinic acid (ALA), sulfonated chloro-aluminum phthalocyanine ($AlPcS_n$), benzoporphyrin derivative monoacid ring A (BPD-MA), and lutetium texaphyrin (Lutex). PDT-induced vascular damage in the chick chorioallantoic membrane (CAM) is measured following topical application of the photosensitizers. In order to make meaningful comparisons, care is taken to keep treatment variables the same. These include light dose (5 and 10 J/cm^2), power density (33 and 100 mW/cm^2), and drug uptake time (30 and 90 min). The drug dose ranges from 0.1 μg/cm^2 for BPD to 5000 μg/cm^2 for ALA. Results are also analyzed statistically according to CAM vessel type (arterioles versus venules), vessel diameter, and vessel development (embryonic age). For each photosensitizer, the order of importance for the various PDT parameters is found to be unique. The differences between the sensitizers are most likely due to variation in biophysical and biochemical characteristics, biodistribution, and uptake kinetics.

Keywords: 5-Aminolevulinic acid (ALA); Benzoporphyrin derivative monoacid ring A (BPD-MA); Lutetium texaphyrin (Lutex); Photodynamic therapy; Photofrin; Sulfonated chloro-aluminum phthalocyanine ($AlPcS_n$); Vascular damage

1. Introduction

Photodynamic therapy (PDT), also called photochemotherapy, is a new modality for the treatment of cancer [1–3] and a variety of nononcologic conditions [3–7]. PDT is based on administering a photosensitizer, which is preferentially retained in tumor (and other proliferating) tissue. When the ratio of photosensitizer concentration present in tumor and surrounding normal tissue is optimal, the tumor area is exposed to light, at a wavelength coinciding with an absorption peak of the photosensitizer (630–800 nm). Photoexcitation of the sensitizer leads to formation of short-lived reactive oxygen intermediaries that are cytotoxic and cause tumor regression, either directly by cell inactivation [8] and/or indirectly by destruction of the tumor vascular microcirculation [9,10].

To date, only Photofrin®, a mixture of porphyrins of partially known composition [11], has received US FDA approval for use in PDT of some selected neoplastic diseases [1]. Unfortunately, Photofrin absorbs weakly at 630 nm and, moreover, is characterized by prolonged cutaneous phototoxicity. Second-generation photosensitizers for improved photochemotherapy are under development and are in various stages of preclinical and clinical trials [1,3].

It is often difficult to compare the in vivo PDT efficacy of different sensitizers. This is because widely dissimilar testing conditions are used, such as different animals, tumor type/location, route of drug administration, time interval between drug and light application, irradiation conditions (light dose and power density), and treatment endpoint. Clearly, it is of interest to compare PDT efficacy of different photosensitizers under identical protocols, using Photofrin as the common reference material.

A few dozen agents are currently being evaluated for their PDT response [12,13]. The present study is limited to four compounds: sulfonated chloro-aluminum phthalocyanine ($AlPcS_n$) [14], benzoporphyrin derivative monoacid ring A (BPD-MA) [15,16], lutetium texaphyrin (Lutex) [17–19], and aminolevulinic acid (ALA), a precursor of the endogenous sensitizer protoporphyrin IX (PpIX) [20]. In Table 1

* Corresponding author. Tel.: +1-949-824-6291; fax: +1-949-824-8413; e-mail: mberns@bli.uci.edu

1011-1344/99/$ - see front matter
PII S1011-1344(99)00124-4

Table 1
In vivo PDT efficacy, relative to that of Photofrin at 630 nm, for selected second-generation sensitizers (data are on a per weight basis and are not corrected for absorbance)

Sensitizer	Relative efficacy	Assay	Tumor or organ	Irradiation (nm)	Reference
$AlPcS_4$	0.7	mouse	C3H	610	[21,22]
$AlPcS_4$	1	mouse	CaD2	675	[23]
$AlPcS_4$	>1	mouse	RIF-1	675	[24]
$AlPcS_4$	2	mouse	SCC	675	[25]
$AlPcS_4$	10	mouse	EMT-6	675	[26]
$AlPcS_4$	1	rat	skin window	675	[27]
$AlPcS_4$	1.2	rat	colon	675	[28]
$AlPcS_4$	0.1 [a]	rat	liver	670	[29]
BPD	10	hamster pouch	SCC	690	[30]
BPD	1.6	mouse	SCCVII	690	[31]
Lutex	1	mouse	C26CC	600–800	[32,33]
Lutex	0.7	mouse	SMT-F	740	[34]
ALA [b]	4	BD9 rat	$LSBD_1$	630	[35]
ALA [b]	5	mouse	C26CC	600-800	[36]
ALA [b]	1	mouse	C26CC	600–800	[33]
ALA [b]	1.2	chicken	comb	630	[37]
ALA [b]	0.8	human	gastrointestinal	628	[38]

[a] Based on ''photodynamic necrosis threshold dose'' [29] and corrected for absorbance.
[b] ALA doses $\times$ 0.01 to compensate for efficiency of bioconversion to PpIX [51].

we present some published results of the PDT efficiency, relative to Photofrin, of these selected sensitizers [21–38].

Because of the importance of the vascular pathway in PDT [9], we have chosen the chick embryo chorioallantoic membrane (CAM) to study vascular effects. The CAM bioassay has two distinct advantages over other animal models. First, it contains a dense capillary plexus supplied by allantoic blood vessels, which allows noninvasive study of in vivo microvasculature and blood circulation together with observation and documentation by video-microscopy. Secondly, it is relatively easy to collect statistically significant data in a fast and efficient way.

For some gynecological [6,39], urological [40], and dermatological [41,42] diseases, topical/intravesical application of sensitizer is preferred. This can be simulated by topical application of drug on the CAM. PDT-induced vascular damage in the CAM using different sensitizers was studied with respect to treatment variables and in vivo conditions.

2. Materials and methods

2.1. Photosensitizers

The following compounds were used without further purification. Stock solutions were prepared in accordance with the manufacturers' specifications.

Porfimer sodium (QLT, Vancouver, Canada), 2.5 mg/ml in 5% dextrose; this preparation is considered to be equivalent to Photofrin.

Sulfonated chloro-aluminum phthalocyanine, $AlPcS_n$ (consisting of a mixture of isomers with $n = 3,4$ sulfonate groups, S) (Ciba–Geigy, Basel, Switzerland), 1 mg/ml in PBS.

5-Aminolevulinic acid, ALA (DUSA Pharmaceuticals, Inc., Denville, NJ), 50 mg/ml in H_2O (adjusted to pH $\approx$ 6), prepared freshly before each experiment.

Benzoporphyrin derivative monoacid, BPD-MA (QLT, Vancouver); the liposomal powder was reconstituted in H_2O, 2 mg/ml. Working solutions were prepared by diluting the stock preparation with 5% dextrose.

Lutetium texaphyrin, Lutex (Compound PCI-0123, Pharmacyclics Inc., Sunnyvale, CA), 2 mg/ml in 5% mannitol.

Photofrin, $AlPcS_n$ and Lutex were stored frozen at -20°C in 1 ml aliquots, used once after thawing; BPD was stored at 4°C for a maximum of three weeks. Working solutions were freshly prepared by dilution with the appropriate solvent.

2.2. CAM preparation

The CAM as an in vivo bioassay for PDT has been described previously [43–47] and was adopted here with minor modifications. Briefly, fertilized chicken eggs were disinfected and transferred to a hatching incubator set at 38°C and 60% humidity. At day four of embryo age (EA 4), 5 ml of albumin was aspired with a 20-gauge needle, through a hole drilled at the narrow apex, to create a false air sac. At EA 7, a 20 mm diameter window was cut into the shell and covered with a sterile Petri dish; incubation was continued in a static incubator.

2.3. Sensitizer application

At EA 12 or 13, when the CAM had matured, 30 μl of sensitizer solution was applied topically in an area demarcated by a Teflon O-ring (6 mm i.d., 1.4 mm annular width) placed aseptically on a well-vascularized site of the CAM.

This defined a 30 mm^2 region of interest on the CAM. Sterile, blackened Petri dishes were placed over the eggshell opening and all further manipulations were performed in subdued light. Prior to irradiation, the sensitizer solution inside the ring area was removed with a pipette and the area was washed twice with 150 μl PBS. This ensured that incident radiation was absorbed by the sensitizer actually taken up by the CAM tissue, without being attenuated through a layer of residual sensitizer solution on the membrane.

2.4. Irradiation parameters

Irradiation wavelengths were 630 nm (with Photofrin and ALA), 675 nm (with phthalocyanine), 690 nm (with BPD), and 729 nm (with Lutex). CW radiation at 630 and 675 nm was delivered by an argon-laser-pumped-dye laser, model CR599 (Coherent, Palo Alto, CA) and at 690 and 729 nm by stacked-diode lasers (Lawrence Livermore Laboratories, Livermore, CA). The laser light was transmitted through a 400 μm multimode fiber, terminated with an uncoated microlens (Miravant Medical Technologies, Santa Barbara, CA), which expanded the beam to cover the whole ring area (60 mm^2, including the annular width). Laser output was determined using a Coherent model 210 power meter. Eggs without photosensitizer were irradiated at each wavelength to determine at which light dose (J/cm^2) damage occurred. All irradiation conditions were well below these light doses. The power density was 33 mW/cm^2 (with 150 or 300 s irradiation time) or 100 mW/cm^2 (with 50 or 100 s irradiation time). With both power densities, the same total light doses (5 and 10 J/cm^2) were obtained, corresponding to energies incident on the CAM surface inside the ring area (30 mm^2) of 1.5 and 3 J.

2.5. PDT

Preliminary experiments were carried out for each sensitizer by visual inspection, to determine the threshold drug dose that causes visible vascular damage in the region of interest at the lower light dose (5 J/cm^2). Groups of five eggs were treated as follows: controls (no drug, no light), dark toxicity (drug only), light sensitivity (irradiation only), and 24 experimental groups using a combination of treatment variables. These included: two light doses (5 and 10 J/cm^2) delivered at two time points (30 and 90 min) after drug application, two power densities (33 and 100 mW/cm^2), and three drug dosages. Thus, at least $2\times2\times2\times3\times5=120$ eggs were used for each drug. For selected combinations of treatment variables, the experiments were repeated using groups of five eggs at embryo age EA 12 or EA 13, different from that of the corresponding treatment group. After irradiation, eggs were covered with blackened Petri dishes and returned to the incubator.

2.6. Video-microscopic documentation

Immediately prior to drug application and also at one hour post-irradiation, the CAM area inside the O-ring was videotaped with a CCD color camera (Sony, model DXC-101) mounted on a stereomicroscope (Olympus, model SZH), using oblique illumination provided by a fiber-optic light guide (Volpi, Switzerland). Final magnification at the TV monitor was 70×. At a later date, videotapes were analyzed, in a double-blind fashion, for quantitation of PDT-induced damage to the CAM microcirculation.

2.7. Damage assessment

The CAM consists of an external layer, derived from the chorion ectoderm, a mesodermal layer containing the extraembryonic vascular network, and an internal layer derived from the allantoic endoderm [43,44]. In the present study we have refined the classification of PDT-induced vascular damage in the CAM mesoderm [45–48]. Careful analysis of video images allowed determination of additional gradations in vascular response. 'Slight damage' was assigned a score 1 or 1.2, 'moderate damage' a score 1.6 or 2, and 'severe damage' a score 2.5 or 3. Damage was also graded according to vessel diameter (d). We assigned the following (arbitrary) weight factors to the damage score: 0 for 'zero-order' capillaries ($d<20$ μm); 1 for 'order-1' venules or arterioles ($d\approx40$ μm); 2 for 'order-2' vessels ($d\approx70$ μm); and 3 for 'order-3' vessels ($d>100$ μm). Typically, the CAM area (≈30 mm^2) inside the ring contained about 75 order-1 blood vessels, 25 order-2 vessels and 10 order-3 vessels, with a slight preponderance of arterioles [43].

For each egg, the weighted damage score was denoted as the highest value of the product 'damage score × vessel-order weight factor', observed in the vasculature of that egg. We have also used this classification to differentiate between the weighted damage scores observed for arterioles and venules. In Table 2 we present the damage classification used in this study (scale 0–9).

In order to utilize only the 'linear' portion of the sigmoid-shaped curve depicting damage score versus treatment variable, the slowly varying portion of the curve near the PDT threshold (with weighted damage scores 0–2) was eliminated by shifting the curve such that scores <2 became zero. For the high-damage portion of the curve (scores 6–9), treatment variables were chosen such that stasis and hemorrhage of 'order-3' vessels, associated with weighted damage scores of 7.5 and 9 respectively, were avoided. The remaining scores 2–6 (Table 2, bold face values) were considered to behave in a linear fashion when comparing treatment variables for a given sensitizer.

The mean damage ± standard error of the mean (SEM) was calculated and the 'effective' damage scores were obtained by subtracting a constant value of two from the mean damage. The downshifted scores defined the 'effective' damage scale, 0–4, used in Figs. 2–4.

Table 2
Weighted damage score for CAM blood vessels

Damage score	Description of damage	Capillary Weight = 0	Order-1 Weight = 1	Order-2 Weight = 2	Order-3 Weight = 3
0	no damage	0	0	0	0
1	coagulation	0	1	**2**	**3**
1.2	vasoconstriction	0	1.2	**2.4**	**3.6**
1.6	coagulation + constriction	0	1.6	**3.2**	**4.8**
2	angiostasis	0	**2**	**4**	**6**
2.5	stasis + vasodilation	0	**2.5**	**5**	7.5
3	hemorrhage	0	**3**	**6**	9

2.8. Choice of treatment variables

In addition to the standard treatment variables (a) drug type, (b) drug dose, (c) light dose and (d) drug uptake time, commonly used in PDT, we have added four more treatment variables, in an effort to more fully elucidate the mechanism(s) of topical PDT. These are (e) power density (less commonly studied in PDT), and three additional variables particularly suited to the CAM model: (f) vessel type (i.e., arterioles and venules), (g) vessel diameter, and (h) embryo age (i.e., vascular development).

(a) The compounds used were second-generation photosensitizers currently under active investigation [1,12,13]. They have different solubilities, span a wide range of photophysical and biochemical properties, and are likely to localize in different subcellular targets.

(b) For topical application on the CAM, three drug dosages were chosen that caused damage in the 'linear' region of the dose–response curve. The selected doses (in units of $\mu g/cm^2$) were BPD 0.1, 0.25, 0.5; Photofrin 1, 2.5, 5; $AlPcS_n$ 1, 2.5, 5; Lutex 5, 10, 25, and ALA 1000, 2500, 5000. It should be noted that ALA requires intracellular conversion to PpIX before becoming photoreactive. Topically applied ALA in humans does not produce a measurable change in the normal systemic levels of porphyrin even when applied at concentrations as high as 200 mg/cm^2 [49], even though localized fluorescence and PDT effects are seen in nearly 100% of the test cases [20]. Measured PpIX concentrations following intravenous [50] or intraperitoneal [51] administration indicate conversion efficiencies in healthy tissues of less than 1%.

(c) Light doses required to elicit vascular response in the CAM model were lower [41] than in other animal systems, because there are no losses due to absorption and scattering of radiation by overlying tissue. We have chosen doses of 5 and 10 J/cm^2, which are about ten times lower than typical light doses used in animal and clinical PDT.

(d) A wide range of drug uptake times is used in PDT. One distinguishes between 'fast'- and 'slow'-acting photosensitizers, having characteristic elimination half-lives ($t_{1/2}$) in plasma. For example, for lipophilic Photofrin $t_{1/2} = 8$ h [52], for PpIX $t_{1/2} = 2$ h [41], for hydrophilic $AlPcS_n$ $t_{1/2} = 1.5$ h [52], whereas for liposomally encapsulated BPD $t_{1/2} = 20$ min [4]. However, with topical application on the CAM, less difference is expected than with systemic administration, since uptake through the extremely thin ectoderm is dominated by diffusion, which is of the same order of magnitude for molecules having similar molecular weights. For the liposomal preparations of BPD, faster diffusion may occur through the ectoderm CAM membrane and, subsequently, through the endothelial cells of blood vessel walls. In order to monitor the time course of uptake for all sensitizers, we have chosen uniform drug-uptake times of 30 and 90 min prior to PDT treatment.

(e) Power densities have been varied to study PDT-induced oxygen depletion [53,54], tissue response to PDT [37,55] or hyperthermia effects [56]. We have used two values (33 and 100 mW/cm^2) and have kept the light dose constant by varying the irradiation time.

(f) Because of the difficulty in determining whether arterioles or venules constitute primary targets, vessel type has been the subject of only few PDT studies; the main findings have been arteriole constriction and venule leakage [57].

(g) Vessel diameters in the CAM range from 20 to 120 mm [43], which encompasses typical diameters of neovasculature in tumors. The vessel diameters have been considered implicitly in the determination of weighted damage scores (Table 2).

(h) The CAM model is characterized by a window of time for experimentation between EA 10, when the CAM is complete, and EA 17, when the embryo becomes immune competent. It is possible to perform vascular PDT from EA 10 onward. However, we selected EA 12 and 13 to make the results relevant for the tumor-bearing CAM. In CAM tumor studies, tumor cells are implanted on EA 8 and the eggs are returned to the incubator until EA 12 or 13, when the tumors are of sufficient size for PDT [58]. They can then be monitored for two more days to determine the PDT efficacy. It should be noted that the CAM is a dynamic system and between EA 12 and 13 the extraembryonic tissues increase in weight by about 15% (from an average of 4.16 g to 4.78 g) [59]. The increase in membrane and/or in vessel-wall thickness may influence drug diffusion across the membrane and increase endothelial cell resistance to PDT-induced damage.

2.9. Statistical analysis

For each sensitizer, statistical analysis of damage scores was performed using a forward stepwise regression analysis to ascertain how well the treatment variables determine vascular damage. In forward stepwise regression, the first treatment variable entered into the regression equation is that with the strongest (positive or negative) correlation with vascular damage. The percentage of variance in vascular damage, which is accounted for by that treatment, is then calculated. The remaining treatment variables are added to the regression equation in successive steps. The stepwise regression algorithm selects the order of entry into the equation such that the treatment that adds the most additional explaining power to the existing regression is added next.

3. Results

Fig. 1 depicts a representative CAM before (a) and after PDT (b), illustrating damage in blood vessels of various diameters. Damage scores for arterioles and venules were measured separately. Table 3 shows the distribution of maximal damage seen for the combined data from all photosensitizers when sorted by vessel type and diameter. In 68% of the CAMs we observed equal damage of arterioles and venules. In the 220 CAMs in which the arteriole and venule damage was unequal, the maximum damage occurred three times more frequently in arterioles (24%) than in venules (8%). This finding is in agreement with rodent studies, where larger PDT effects were observed in arteries as opposed to veins [57,60]. Breakdown of the distribution of maximal damage into photosensitizer groups gave similar patterns for each photosensitizer, with the exception of BPD. With BPD 15% of the CAMs had more venous maximal damage, 9% had more arterial maximal damage, and 76% had equal arterial and venous damage.

The size of a vessel appears to be more important than its type (arteriole or venule) as a predictor of its potential for

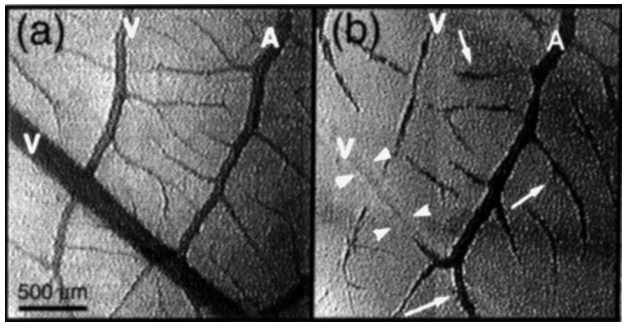

Fig. 1. Video-micrographs of CAM vasculature before (a) and after (b) BPD-mediated PDT. Major arterial (A) and venous (V) vessels are indicated. In (b) the arrows denote points of hemorrhage and the arrowheads indicate the location of the empty large vein. The arterial tree is static and vasodilated while aggregates of red blood cells continue to pass through the venous tree. For PDT the CAM was treated with 0.5 μg/cm^2 BPD for 30 min prior to being irradiated with 690 nm light (33 mW/cm^2, 10 J/cm^2).

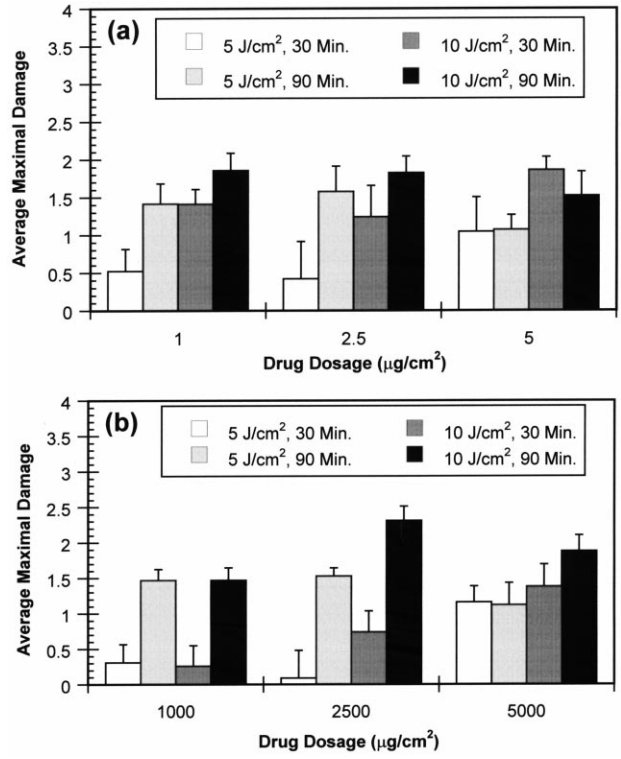

Fig. 2. Maximal 'effective' damage in CAM vasculature with light dose and drug uptake time as dominant treatment variables: (a) Photofrin-based PDT; (b) ALA-based PDT.

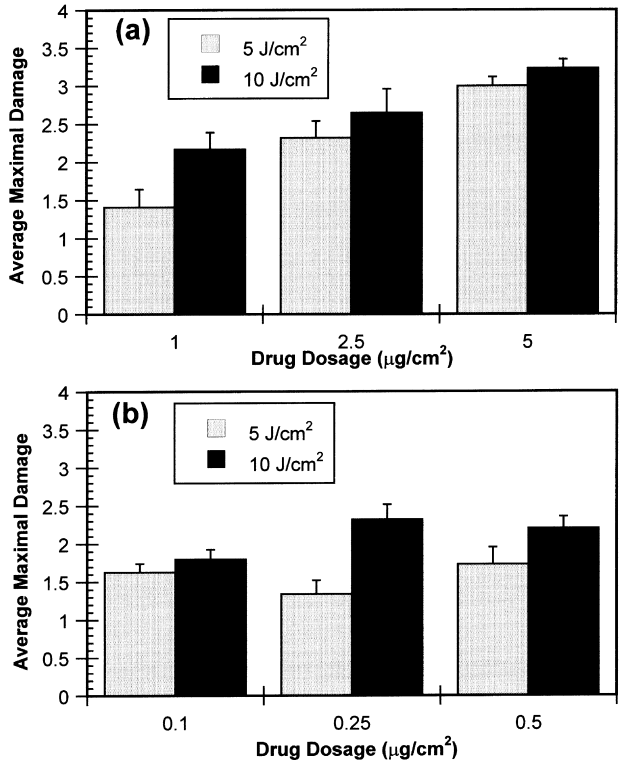

Fig. 3. Maximal 'effective' damage in CAM vasculature with light dose as dominant treatment variable: (a) AlPcS$_n$-based PDT; (b) BPD-based PDT.

undergoing PDT damage. Table 3 clearly shows that 'order-2 vessels' are the most likely to be damaged. Although they

Table 3
Number of CAMs showing maximal damage in vessels of order-*n*

Vessel order (frequency)	Order-1 (69%)	Order-2 (23%)	Order-3 (8%)
Diameter (μm)	$d \approx 40$	$d \approx 70$	$d \geq 100$
Arteriole = venule damage	47 (7%)	419 (61%)	
Arteriole > venule damage	19 (3%)	136 (20%)	7 (1%)
Venule > arteriole damage	7 (1%)	51 (7%)	0 (0)
Aggregate order-*n* damage	73 (11%)	606 (88%)	7 (1%)

represent only 23% of the vessels present in the average region of interest [43], they account for 88% of the maximally damaged vessels. It should be noted that for a maximal damage score in any one vessel of 'order-*n*', many other vessels of that order or of 'order $n-1$' may have received the same (or a lower) damage score. It is noteworthy that of all 'order-3' vessels, only seven arterioles, representing seven CAMs, contributed to the maximum damage scores (i.e., about 1% of all CAMs). For the remainder of the analysis, arterioles and venules were grouped together and the higher of the two damage scores was recorded.

Embryo age (EA) was an important variable only for Photofrin, where it explained 9% of the total variance in damage. For simplicity, we have combined corresponding data obtained at different embryo ages EA 12 and EA 13.

Table 4 shows the contributions of four treatment variables:drug dose, light dose, power density, and drug uptake time. Since each row of the Table displays the results of a forward stepwise regression analysis, the numbers in a row are order dependent. At each step, the percentage of vascular damage attributed to a particular treatment variable was calculated, starting with the largest, i.e., the most important treatment variable for that sensitizer. Thus the largest number in a row is the percentage of damage with that sensitizer accounted for by that treatment variable. The second-largest number in a row is the percentage of *additional* variance accounted for by the addition of that treatment variable to the regression equation, and so forth.

The bar graphs, Figs. 2–4, include the two or three treatment variables of primary importance to the damage score (Table 4, bold face). The remaining variables, which are of secondary importance, were ignored. An exception to this rule was the inclusion of drug dose as a determining treatment variable, even if not justified by the analysis (as in the case of Photofrin), in order to allow drug dosages to be plotted on the abscissa in a uniform fashion. Figs. 2–4 present the mean 'effective' damage ± SEM, induced in the CAM vasculature by the five photosensitizers as a function of drug dose and of one or two of the most influential treatment variables.

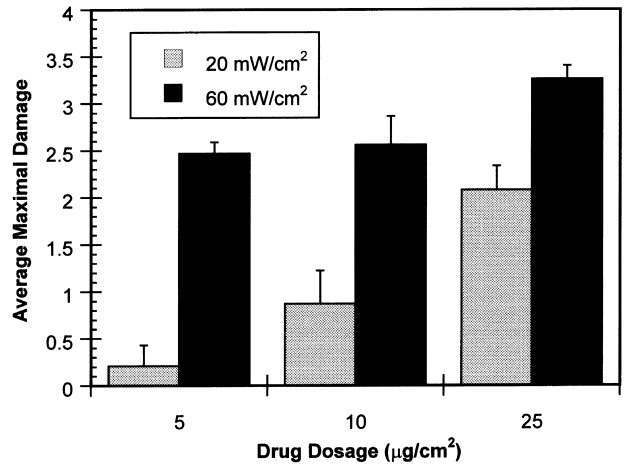

Fig. 4. Maximal 'effective' damage in CAM vasculature with power density as dominant treatment variable for Lutex-based PDT.

The number of eggs analyzed per group depended on the number of treatment variables considered to be important; i.e., 10 eggs per group for Photofrin and ALA (Fig. 2) and 20 eggs per group for $AlPcS_n$, BPD, and Lutex (Figs. 3 and 4).

In Fig. 5, the percentage of variance accounting for the vascular damage explained by an individual treatment variable is proportional to the height of the corresponding section in the stacked bar graph. For each sensitizer, the total percentage that could be explained using all four treatment variables is given by the bar height and ranged from 11% for BPD to 54% for Lutex.

4. Discussion

The photosensitizers chosen for this study ranged from predominantly lipophilic (Photofrin), through amphiphilic (BPD) to hydrophilic (ALA, $AlPcS_n$, and Lutex). This influenced uptake characteristics, since the degree of hydrophilicity of a photosensitizer and the clearance kinetics from blood plasma determine the rate of accumulation in the CAM vasculature. For example, Fig. 5 shows a relatively large influ-

Table 4
Percentage of damage of CAM blood vessels explained by the treatment variables (from stepwise regression). Treatment variables retained in Figs. 2–4 to explain topical PDT damage are given in bold face

Sensitizer	Drug dose	Light dose	Power density	Uptake time	Total percentage accounted for
Photofrin	0.9	**7.3**	3.6	**5.1**	16.9
ALA	2.3	**2.5**	1.3	**21.3**	27.4
$AlPcS_n$	**22.9**	**4.6**	1.1	0.1	28.7
BPD	**1.2**	**9.4**	0.1	0.4	11.1
Lutex	**11.9**	1.9	**39.8**	0.2	53.8

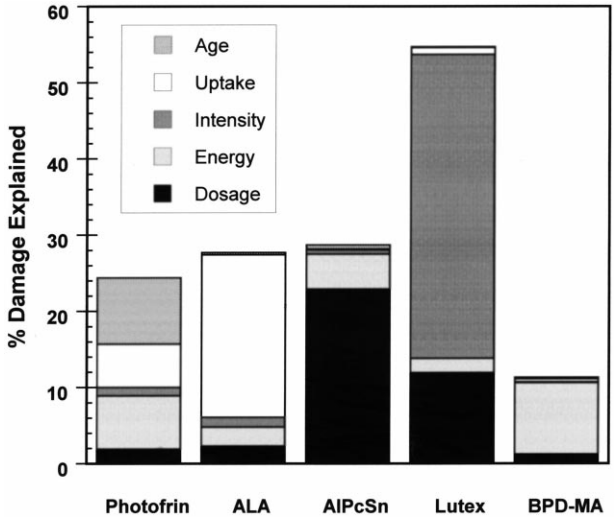

Fig. 5. Percentage of variance accounting for vascular damage, following PDT mediated by different photosensitizers, as explained by five treatment variables.

ence of uptake time for Photofrin. This may be due to the fact that Photofrin is taken up more slowly [52] than the other sensitizers used in this study. In fact, for the relatively short uptake times (up to 90 min) in the present study, the uptake kinetics was rate limiting. As a result, vascular damage depended little on the actual drug dose, which ranged from 'low' ($1\ \mu g/cm^2$) through 'medium' ($2.5\ \mu g/cm^2$) to 'high' ($5\ \mu g/cm^2$). Similarly, uptake time was important for ALA. The accumulation of PpIX, presumably in the mitochondria of endothelial cells [61] of the CAM vasculature, required additional time after cellular uptake of ALA for the intracellular conversion to PpIX. Dependencies on the remaining treatment variables can be understood in a similar fashion [62]. The power density was significant only with Lutex, which may be related [34] to a higher sensitivity to heat generation, noting that hyperthermia is known to play a role in PDT [33,47,56,63].

Based on the statistical analysis of five regression equations, we can rank the treatment variables according to their importance in explaining the observed vascular damage, as listed in Table 4:

Drug dose $\text{AlPcS}_n \gg \text{Lutex} \gg \text{ALA} > \text{BPD} \approx \text{Photofrin}$

Light dose $\text{BPD} > \text{Photofrin} > \text{AlPcS}_n > \text{ALA} > \text{Lutex}$

Power density $\text{Lutex} \gg \text{Photofrin} > \text{ALA} \approx \text{AlPcS}_n > \text{BPD}$

Uptake time $\text{ALA} \gg \text{Photofrin} \gg \text{BPD} \approx \text{Lutex} \approx \text{AlPcS}_n$

It is apparent from the preceding summary that the photosensitizers tested vary widely in their response to treatment variables, including those commonly investigated; e.g., drug and light dose and drug–light time interval. An important finding is that for Lutex, treatment variables that have not been investigated extensively (e.g., power density) may play a larger role than previously thought. For BPD, the treatment variables considered were capable of accounting for only a small percentage of the variance in damage. This may point to a special role being played by its amphiphilicity or by its liposomal encapsulation [12,13]. Additional work needs to be done before the implications of these findings for a better understanding of the mechanisms of PDT become clear. However, these results do establish that different treatment variables, including some lesser-studied ones such as power density, are more important for certain sensitizers than for others.

This study was focused on the vascular effects of topically applied photosensitizers in the non-tumor-bearing CAM. Because of similar size and developmental characteristics of the neovasculature in the CAM and in tumors, our results have relevance to in vivo PDT. A separate investigation is under way in which sensitizers are administered systemically in the chick embryo. This is relevant for clinical PDT mediated by i.p.- or i.v.-administered agents. Future studies will examine PDT of the tumor-bearing CAM, which will allow us to compare the importance of cellular versus vascular pathways of PDT in a controlled model system that approximates the in vivo situation more closely.

5. Abbreviations

ALA	5-aminolevulinic acid
AlPcS_n	sulfonated chloro-aluminum phthalocyanine
BPD-MA	benzoporphyrin derivative monoacid
CAM	chorioallantoic membrane
EA	embryo age
Lutex	lutetium texaphyrin
PpIX	protoporphyrin IX

Acknowledgements

The authors thank Jonathan Eusebio for valuable technical assistance. Dr Anita L. Iannucci, UCI Center for Statistical Consulting, performed the statistical analysis. Institutional support from the Office of Naval Research (N00014-94-1-0874), the Department of Energy (DE-FG03-91ER61227), National Institutes of Health 5R01 CA 32248-14 (RR-01192), and the Beckman Laser Institute and Medical Clinic Endowment is also gratefully acknowledged. S.K. received partial support from the US–Israel Binational Science Foundation, grant 93-00154.

References

[1] T.J. Dougherty, C.J. Gomer, B.W. Henderson, G. Jori, D. Kessel, M. Korbelik, J. Moan, Q. Peng, Photodynamic therapy, J. Natl. Cancer Inst. 90 (1998) 889–905.
[2] J.J. Schuitmaker, P. Baas, H.L.L.M. van Leengoed, F.W. van der Meulen, W.M. Star, N. van Zandwijk, Photodynamic therapy: a promising new modality for the treatment of cancer, J. Photochem. Photobiol. B: Biol. 34 (1996) 3–12.
[3] A.M.R. Fisher, A.L. Murphree, C.J. Gomer, Clinical and preclinical photodynamic therapy, Lasers Surg. Med. 17 (1995) 2–31.

[4] K.B. Trauner, R. Gandour-Edwards, M. Bamberg, S. Shortkroff, C. Sledge, T. Hasan, Photodynamic synovectomy using benzoporphyrin derivative in an antigen-induced arthritis model for rheumatoid arthritis, Photochem. Photobiol. 67 (1998) 133–139.
[5] S. Asrani, S. Zou, S. D'Anna, G. Lutty, S.A. Vinores, M.F. Goldberg, R. Zeimer., Feasibility of laser-targeted photoocclusion of the choriocapillary layer in rats, Invest. Ophthalmol. 38 (1997) 2702–2710.
[6] R.A. Steiner, Y. Tadir, B.J. Tromberg, T. Krasieva, A.T. Gazains, P. Wyss, M.W. Berns, Photosensitization of the rat endometrium following 5-aminolevulinic acid induced photodynamic therapy, Lasers Surg. Med. 18 (1996) 301–308.
[7] K.W. Woodburn, Q. Fan, D. Kessel, M. Wright, T.D. Mody, G. Hemmi, D. Magda, J.L. Sessler, W.C. Dow, R.A. Miller, S.W. Young, Phototherapy of cancer and atheromatous plaque with texaphyrins, J. Clin. Laser Med. Surg. 14 (1996) 343–348.
[8] R. Hilf, Cellular targets of photodynamic therapy, in: B.W. Henderson, T.J. Dougherty (Eds.), Photodynamic Therapy. Basic Principles and Clinical Applications, Marcel Dekker, New York, 1992, pp. 47–54.
[9] W.M. Star, P.A. Marijnissen, A.E. van den Berg-Blok, J.A.C. Versteeg, K.A.P. Franken, H.S. Reinhold, Destruction of rat mammary tumor and normal tissue microcirculation by hematoporphyrin derivative photoradiation observed in vivo in sandwich observation chambers, Cancer Res. 46 (1986) 2532–2540.
[10] J.S. Nelson, L.H. Liaw, A. Orenstein, W.G. Roberts, M.W. Berns, Mechanism of tumor destruction following photodynamic therapy with hematoporphyrin derivative, chlorin, and phthalocyanine, J. Natl. Cancer Inst. 80 (1988) 1599–1605.
[11] D. Kessel, C.J. Byrne, A.D. Ward, Photosensitizing dyes related to hematoporphyrin derivative: structure-activity relationships, in: B.W. Henderson, T.J. Dougherty (Eds.), Photodynamic Therapy. Basic Principles and Clinical Applications, Marcel Dekker, New York, 1992, pp. 129–143.
[12] R.W. Boyle, D. Dolphin, Structure and biodistribution relationships of photodynamic sensitizers, Photochem. Photobiol. 64 (1996) 469–485.
[13] G. Jori, Tumour photosensitizers: approaches to enhance the selectivity and efficiency of photodynamic therapy, J. Photochem. Photobiol. B: Biol. 36 (1996) 87–93.
[14] B. Paquette, J.E. van Lier, Phthalocyanines and related compounds: structure-activity relationships, in: B.W. Henderson, T.J. Dougherty (Eds.), Photodynamic Therapy. Basic Principles and Clinical Applications, Marcel Dekker, New York, 1992, pp. 145–156.
[15] B.A. Allison, E. Waterfield, A.M. Richter, J.G. Levy, The effects of plasma lipoproteins on in vitro tumor cell killing and in vivo tumor photosensitization with benzoporphyrin derivative, Photochem. Photobiol. 54 (1991) 709–715.
[16] A.M. Richter, E. Waterfield, A.K. Jain, A.J. Canaan, B.A. Allison, J.G. Levy, Liposomal delivery of a photosensitizer, benzoporphyrin derivative monoacid ring A (BPD), to tumor tissue in a mouse tumor model, Photochem. Photobiol. 57 (1993) 1000–1006.
[17] S.W. Young, K.W. Woodburn, M. Wright, T.D. Mody, Q. Fan, J.L. Sessler, W.C. Dow, R.A. Miller, Lutetium texaphyrin (PCI-0123): a near-infrared, water-soluble photosensitizer, Photochem. Photobiol. 63 (1996) 892–897.
[18] K.W. Woodburn, Q. Fan, D.R. Miles, D. Kessel, Y. Luo, S.W. Young, Localization and efficacy analysis of the phototherapeutic lutetium texaphyrin (PCI-0123) in the murine EMT6 sarcoma model, Photochem. Photobiol. 65 (1997) 410–415.
[19] K.W. Woodburn, Q. Fan, D. Kessel, Y. Luo, S.W. Young, Photodynamic therapy of B16F10 murine melanoma with lutetium texaphyrin, J. Invest. Dermatol. 110 (1998) 746–751.
[20] J.C. Kennedy, R.H. Pottier, Endogenous protoporphyrin IX, a clinically useful photosensitizer for photodynamic therapy, J. Photochem. Photobiol. B: Biol. 14 (1992) 275–292.
[21] J.F. Evensen, J. Moan, A test of different photosensitizers for photodynamic treatment of cancer in a murine tumor model, Photochem. Photobiol. 46 (1987) 859–865.
[22] J. Moan, Q. Peng, J.F. Evensen, K. Berg, A. Western, C. Rimington, Photosensitizing efficiencies, tumor- and cellular uptake of different photosensitizing drugs relevant for photodynamic therapy of cancer, Photochem. Photobiol. 46 (1987) 713–721.
[23] Q. Peng, J. Moan, Correlation of distribution of sulphonated phthalocyanines with their photodynamic effect in tumour and skin of mice bearing CaD2 mammary carcinoma, Br. J. Cancer 72 (1995) 565–574.
[24] S.A.A. Zaidi, N.L. Oleinick, M.T. Zaim, H. Mukhtar, Apoptosis during photodynamic therapy-induced ablation of RIF-1 tumors in C3H mice: electron microscopic, histopathologic and biochemical evidence, Photochem. Photobiol. 58 (1993) 771–776.
[25] K. Koshida, H. Hisazumi, K. Komatsu, A. Hirata, T. Uchibayashi, Possible advantages of aluminum-chloro-tetrasulfonated phthalocyanine over hematoporphyrin derivative as a photosensitizer in photodynamic therapy, Urol. Res. 21 (1993) 283–288.
[26] J.S. Nelson, W.G. Roberts, L.H. Liaw, M.W. Berns, Cellular and tumor model studies using several PDT sensitizers, in: D. Kessel (Ed.), Photodynamic Therapy of Neoplastic Disease, vol. 1, CRC Press, Boca Raton, FL, 1990, pp. 147–168.
[27] S.J. Stern, S. Flock, S. Small, S. Thomsen, S. Jacques, Chloroaluminum sulfonated phthalocyanine versus dihematoporphyrin ether: early vascular events in the rat window chamber, Laryngoscope 101 (1991) 1219–1225.
[28] H. Barr, A.J. MacRobert, C.J. Tralau, P.B. Boulos, S.G. Bown, The significance of the nature of the photosensitiser for photodynamic therapy: quantitative and biological studies in the colon, Br. J. Cancer 62 (1990) 730–735.
[29] T.J. Farrell, B.C. Wilson, M.S. Patterson, M.C. Olivo, Comparison of the in vivo photodynamic threshold dose for Photofrin, mono- and tetrasulfonated aluminum phthalocyanine using a rat liver model, Photochem. Photobiol. 68 (1998) 394–399.
[30] A.W. Hemming, N.L. Davis, B. Dubois, N.F. Quenville, R.J. Finley, Photodynamic therapy of squamous cell carcinoma. An evaluation of a new photosensitizing agent, benzoporphyrin derivative and new photoimmunoconjugate, Surg. Oncol. 2 (1993) 187–196.
[31] M. Korbelik, G. Krosl, Cellular levels of photosensitizers in tumours: the role of proximity to the blood supply, Br. J. Cancer 70 (1994) 604–610.
[32] G. Kostenich, A. Orenstein, L. Roitman, Z. Malik, B. Ehrenberg, In vivo photodynamic therapy with the new near-IR absorbing water soluble photosensitizer lutetium texaphyrin and a high fluence rate pulsed light delivery system, J. Photochem. Photobiol. B: Biol. 39 (1997) 36–42.
[33] G. Kostenich, A. Orenstein, Z. Malik, B. Ehrenberg, Preclinical photodynamic therapy studies with endogenous and new exogenous photosensitizers, in: J.G. Moser (Ed.), Photodynamic Tumor Therapy, Harwood, Amsterdam, 1998, pp. 101–114.
[34] M.J. Hammer-Wilson, M. Ghahramanlou, M.W. Berns, Photodynamic activity of lutetium-texaphyrin in a mouse tumor system, Lasers Surg. Med. 24 (1999) 276–284.
[35] F. Cairnduff, D.J.H. Roberts, B. Dixon, S.B. Brown, Response of a rodent fibrosarcoma to photodynamic therapy using 5-aminolaevulinic acid (ALA) or polyhaematoporphyrin, Int. J. Radiat. Biol. 67 (1995) 93–99.
[36] A. Orenstein, G. Kostenich, L. Roitman, Y. Shechtman, Y. Kopolovic, B. Ehrenberg, Z. Malik, A comparative study of tissue distribution and photodynamic therapy selectivity of chlorin e6, Photofrin II, and ALA-induced protoporphyrin XI in a colon carcinoma model, Br. J. Cancer 73 (1996) 937–944.
[37] C.J. Chang, C.H. Sun, L.H.L. Liaw, M.W. Berns, J.S. Nelson, In vitro and in vivo photosensitizing capabilities of 5-ALA versus Photofrin in vascular endothelial cells, Lasers Surg. Med. 24 (1999) 178–186.
[38] P. Mlkvy, H. Messmann, J. Regula, M. Conio, M. Pauer, C.E. Millson, A.J. MacRobert, S.G. Bown, Photodynamic therapy for gastrointestinal tumors using three photosensitizers — ALA induced PPIX, Photofrin and MTHPC. A pilot study, Neoplasma 45 (1998) 157–161.

[39] P. Hillemanns, M. Korell, M. Schmitt-Sody, R. Baumgartner, W. Beyer, R. Kimmig, M. Untch, H. Hepp, Photodynamic therapy in women with cervical intraepithelial neoplasia using topically applied 5-aminolevulinic acid, Int. J. Cancer 81 (1999) 34–38.
[40] S.C. Chang, G. Buonaccorsi, A.J. MacRobert, S.G. Bown, 5-Aminolevulinic acid (ALA)-induced protoporphyrin IX fluorescence and photodynamic effects in the rat bladder: an in vivo study comparing oral and intravesical ALA administration, Lasers Surg. Med. 20 (1997) 252–264.
[41] Q. Peng, T. Warloe, K. Berg, J. Moan, M. Kongshaug, K.E. Giercksky, J.M. Nesland, 5-Aminolevulinic acid-based photodynamic therapy. Clinical research and future challenges, Cancer 79 (1997) 2282–2308.
[42] A. Orenstein, G. Kostenich, Z. Malik, The kinetics of protoporphyrin fluorescence during ALA-PDT in human malignant skin tumors, Cancer Lett. 120 (1997) 229–234.
[43] D.O. DeFouw, V.J. Rizzo, R. Steinfeld, R.N. Feinberg, Mapping of the microcirculation in the chick chorioallantoic membrane during normal angiogenesis, Microvasc. Res. 38 (1989) 333–336.
[44] A. Fuchs, E.S. Lindenbaum, The two- and three-dimensional structure of the microcirculation of the chick chorioallantoic membrane, Acta Anat. 131 (1988) 271–275.
[45] V. Gottfried, E.S. Lindenbaum, S. Kimel, Vascular damage during PDT as monitored in the chick chorioallantoic membrane, Int. J. Radiat. Biol. 60 (1991) 349–354.
[46] V. Gottfried, R. Davidi, C. Averbuj, S. Kimel, In vivo damage to chorioallantoic membrane blood vessels by porphycene-induced photodynamic therapy, J. Photochem. Photobiol. B: Biol. 30 (1995) 115–121.
[47] S. Kimel, L.O. Svaasand, M. Hammer-Wilson, V. Gottfried, S. Cheng, E. Svaasand, M.W. Berns, Demonstration of synergistic effects of hyperthermia and photodynamic therapy using the chick chorioallantoic membrane model, Lasers Surg. Med. 12 (1992) 432–440.
[48] S. Kimel, L.O. Svaasand, M. Hammer-Wilson, M.J. Schell, T.E. Milner, J.S. Nelson, M.W. Berns, Differential vascular response to laser photothermolysis, J. Invest. Dermatol. 103 (1994) 693–700.
[49] C. Fritsch, J. Batz, K. Bolsen, T. Ruzicka, G. Goerz, Influence of topical photodynamic therapy with 5-aminolevulinic acid on porphyrin metabolism, Arch. Dermatol Res. 288 (1996) 517–521.
[50] C.S. Loh, D. Vernon, A.J. MacRobert, J. Bedwell, S.G. Bown, S.B. Brown, Endogenous porphyrin distribution induced by 5-aminolaevulinic acid in the tissue layers of the gastrointestinal tract, J. Photochem. Photobiol. B: Biol. 20 (1993) 47–54.
[51] B.W. Henderson, L. Vaughan, D.A. Bellnier, H. van Leengoed, P.G. Johnson, A.R. Oseroff, Photosensitization of murine tumor, vasculature, and skin by using 5-aminolevulinic acid-induced porphyrin, Photochem. Photobiol. 62 (1995) 780–789.
[52] Q. Peng, J. Moan, M. Kongshaug, J.F. Evensen, H. Anholt, C. Rimington, Sensitizer for photodynamic therapy of cancer: a comparison of the tissue distribution of Photofrin I and aluminum phthalocyanine tetrasulfonate in nude mice bearing a human malignant tumor, Int. J. Cancer 48 (1991) 258–264.
[53] R. Sorensen, V. Iani, J. Moan, Kinetics of photobleaching of protoporphyrin IX in the skin of nude mice exposed to different fluence rates of red light, Photochem. Photobiol. 68 (1998) 835–840.
[54] T.M. Sitnik, J.A. Hampton, B.W. Henderson, Reduction of tumour oxygenation during and after photodynamic therapy in vivo: effects of fluence rate, Br. J. Cancer 77 (1998) 1386–1394.
[55] T.M. Sitnik, B.W. Henderson, The effect of fluence rate on tumor and normal tissue responses to photodynamic therapy, Photochem. Photobiol. 67 (1998) 462–466.
[56] M. Uehara, T. Inokuchi, K. Sano, Experimental study of combined hyperthermic and photodynamic therapy on carcinoma in the mouse, J. Oral Maxillofac. Surg. 54 (1996) 729–736.
[57] V.H. Fingar, T.J. Wieman, S.A. Wiehle, P.B. Cerrito, The role of microvascular damage in photodynamic therapy: the effect of treatment on vessel constriction, permeability, and leukocyte adhesion, Cancer Res. 52 (1992) 4914–4921.
[58] R. Hornung, M.J. Hammer-Wilson, S. Kimel, L.H. Liaw, Y. Tadir, M.W. Berns, Systemic application of photosensitizers in the chick chorioallantoic membrane (CAM) model: Photodynamic response of CAM vessels and 5-aminolevulinic acid uptake kinetics by transplantable tumors, J. Photochem. Photobiol. B: Biol. 49 (1999) 41–49.
[59] A.L. Romanoff, A.J. Romanoff, Biochemistry of the Avian Embryo: a Quantitative Analysis of Prenatal Development, Interscience Publishers, New York, 1967, p. 341.
[60] M.W. Reed, T.J. Wieman, D.A. Schuschke, F.N. Miller, A comparison of the effects of photodynamic therapy on normal and tumor blood vessels in the rat microcirculation, Radiat. Res. 119 (1989) 542–552.
[61] L. Gibson, J.J. Havens, T.H. Foster, R. Hilf, Time-dependent intracellular accumulation of delta-aminolevulinic acid, induction of porphyrin synthesis and subsequent phototoxicity, Photochem. Photobiol. 65 (1997) 416–421.
[62] J.W. Winkelman, S. Kimel, The relationship between porphyrin transport and tissue uptake with photosensitization from $^1O_2$, in: D. Kessel (Ed), Photodynamic Therapy of Neoplastic Disease, vol. 2, CRC Press, Boca Raton, FL, 1990, pp. 29–42.
[63] D.L. Liu, S. Andersson-Engels, C. Sturesson, K. Svanberg, C.H. Hakansson, S. Svanberg, Tumor vessel damage resulting from laser-induced hyperthermia alone and in combination with photodynamic therapy, Cancer Lett. 111 (1997) 157–165.